HHS Public Access

Author manuscript

Nat Med. Author manuscript; available in PMC 2019 January 02.

Published in final edited form as:

Nat Med. 2018 August ; 24(8): 1151–1156. doi:10.1038/s41591-018-0082-y.

DPP8/9 inhibitor-induced pyroptosis for treatment of acute myeloid leukemia

Darren C. Johnson[1,#], **Cornelius Y. Taabazuing**[2,#], **Marian C. Okondo**[2], **Ashley J. Chui**[1], **Sahana D. Rao**[1], **Fiona C. Brown**[3], **Casie Reed**[3], **Elizabeth Peguero**[4], **Elisa de Stanchina**[4], **Alex Kentsis**[1,3,5,6], and **Daniel A. Bachovchin**[1,2,6,*]

[1]Tri-institutional PhD Program in Chemical Biology, Memorial Sloan Kettering Cancer Center, New York, New York, USA

[2]Chemical Biology Program, Memorial Sloan Kettering Cancer Center, New York, New York, USA

[3]Molecular Pharmacology Program, Memorial Sloan Kettering Cancer Center, New York, New York, USA

[4]Antitumor Assessment Facility, Memorial Sloan Kettering Cancer Center, New York, New York, USA

[5]Department of Pediatrics, Memorial Sloan Kettering Cancer Center, New York, New York, USA

[6]Pharmacology Program of the Weill Cornell Graduate School of Medical Sciences, Memorial Sloan Kettering Cancer Center, New York, New York, USA

Abstract

Small-molecule inhibitors of the serine dipeptidases DPP8 and DPP9 (DPP8/9) induce a lytic form of cell death called pyroptosis in mouse and human monocytes and macrophages[1,2]. In mouse myeloid cells, Dpp8/9 inhibition activates the inflammasome sensor Nlrp1b, which in turn activates pro-caspase-1 to mediate cell death[3], but the mechanism of DPP8/9 inhibitor-induced pyroptosis in human myeloid cells is not yet known. Here we show that the CARD-containing protein CARD8 mediates DPP8/9 inhibitor-induced pro-caspase-1 dependent pyroptosis in human myeloid cells. We further show that DPP8/9 inhibitors induce pyroptosis in the large majority of human acute myeloid leukemia (AML) cell lines and primary AML samples, but not in cells from many other lineages, and that these inhibitors inhibit human AML progression in mouse models. Overall, this work identifies the first known activator of CARD8 in human cells and indicates that

*Correspondence to: bachovcd@mskcc.org.
#Equal contribution

AUTHOR CONTRIBUTIONS

D.A.B. conceived and directed the project, performed experiments, and analyzed data, and wrote the paper; D.C.J., C.Y.T, M.C.O., A.J.C., and S.D.R. performed experiments and analyzed data; D.C.J., M.C.O., F.C.B., C.R. and E. P. performed xenograft experiments; E.d.S. advised the xenograft experiments. A.K. provided cell biology, mouse xenograft and leukemia expertise.

COMPETING FINANCIAL INTERESTS STATEMENT

The authors declare no competing financial interests.

DATA AVAILABILITY

All relevant data are available upon reasonable request to the corresponding author.

its activation by small-molecule DPP8/9 inhibitors represents a new potential therapeutic strategy for AML.

Val-boroPro (Fig. 1a, also called PT-100 and Talabostat) is a non-selective inhibitor of the post-proline cleaving serine proteases[4–6] that induces anti-cancer immune responses in syngeneic mouse tumor models[7,8]. In mice, Val-boroPro increases the serum protein levels of several cytokines, including G-CSF and Cxcl1, and these cytokines are thought to drive tumor-specific immunity[7]. We recently discovered that inhibition of two intracellular serine dipeptidases Dpp8 and Dpp9 (Dpp8/9) by Val-boroPro activates the inflammasome sensor protein Nlrp1b in murine macrophages, which in turn activates pro-caspase-1 and triggers a lytic form of cell death known as pyroptosis[1,3]. This pathway is essential for the immunostimulatory activity of Val-boroPro in mice, as Val-boroPro does not elevate serum cytokines in either *Casp1*$^{-/-}$ and *Nlrp1b*$^{-/-}$ animals. Based on the promising anti-tumor results in mice, Val-boroPro was tested as a potential immuno-oncology agent in human clinical trials more than a decade ago[9–11]. Val-boroPro elevated the levels of a number of cytokines, including G-CSF, in both healthy volunteers and cancer patients[9], demonstrating that Val-boroPro also activates human immune systems. We recently reported that, as in mice, Val-boroPro also induces pro-caspase-1-dependent pyroptosis in human THP-1 monocytes[1]. However, it remains unknown how DPP8/9 inhibition activates pro-caspase-1 in humans and if this pathway can be harnessed for therapeutic benefit.

Because DPP8/9 inhibitors are cytotoxic to THP-1 cells, which are monocytic cancer cells cultured from the blood of a patient with AML, but not to many other cell types[1,7], we hypothesized that DPP8/9 inhibition might be a specific vulnerability for AML cells. Val-boroPro is the most potent known inhibitor of DPP8 and DPP9[12], and correspondingly is also the most potent known activator of DPP8/9 inhibitor-induced pyroptosis[1]. We therefore first evaluated the activity of Val-boroPro across a panel of cancer cell lines (Fig. 1b,c). Consistent with our hypothesis, 12 of the 17 AML cell lines tested were sensitive to Val-boroPro as determined by CellTiter-Glo, with IC_{50} values ranging from 6 to 206 nM (Supplementary Table 1). Sensitive AML cells treated with Val-boroPro released the cytoplasmic enzyme lactate dehydrogenase (LDH) into the supernatant and stained positive for Annexin V and propidium iodide (Supplementary Fig. 1), confirming that Val-boroPro was indeed inducing lytic cell death. Val-boroPro had no activity against any of the non-AML cell lines tested (Fig. 1c, Supplementary Table 2).

Val-boroPro inhibits DPP4 and DPP7 in addition to DPP8/9[1]. To confirm that these cytotoxic responses were due to DPP8/9 inhibition, we next tested two additional, albeit less potent, DPP8/9 inhibitors, L-*allo*-Ile-isoindoline[12] and 1G244[13,14], across this cell line panel (Supplementary Figs. 2 and 3). Importantly, these two compounds are structurally unrelated to Val-boroPro and are selective for DPP8/9 over DPP4 and DPP7 [1,15]. As expected, the AML cell lines that were sensitive to Val-boroPro were also sensitive to these compounds (Supplementary Fig. 3a,b, Supplementary Table 1). In contrast, these cell lines were not sensitive to the selective DPP4 inhibitor sitagliptin or the selective DPP7 inhibitor 5385[1] (Supplementary Fig. 3c,d), nor did these compounds augment the cytotoxicity of a selective DPP8/9 inhibitor (Supplementary Fig. 3e). Consistent with this inhibitor data, *DPP9*

knockout induced spontaneous lytic cell death in THP-1 cells[1], and this effect was slightly increased in *DPP8/9* double knockout cells. Val-boroPro induced no additional cell death in *DPP8/9* knockout THP-1 cells, indicating that DPP8/9 are the key targets in these human cells. We were unable to isolate *DPP9* knockout MV4;11 or MOLM-13 cells, consistent with their increased sensitivities to Val-boroPro relative to THP-1 cells (Supplementary Fig. 4a). In contrast, *DPP9* knockout A375 cells did not spontaneously undergo lytic cell death (Supplementary Fig. 4b,c). It should be noted that vildagliptin, a potent inhibitor of DPP4 and a weak inhibitor of DPP8/9, was previously reported to synergize with parthenolide to kill AML cells[16]. However, vildagliptin did not exhibit any anti-AML cytotoxicity on its own[16], consistent with its low affinity for DPP8/9. The mechanistic basis for its synergy with parthenolide, including whether caspase-1 and pyroptosis are involved, was not examined in this work and to date remains unknown.

Even though all of the sensitive AML cell lines responded to Val-boroPro, the extent of cell death at 48 h varied between these lines (Fig. 1b). For example, several cell lines had >80% reduction in cell viability (MV4;11, OCI-AML2, SET-2, RS4;11, and MOLM-13), while others had only a 40–65% reduction in viability (KG1, THP-1, and NOMO-1). We speculated that these differences might reflect varying rates of pyroptosis induction, and we therefore assayed cell viability over five days (Fig. 1d–f, Supplementary Fig. 5). Consistent with this premise, MV4;11 and OCI-AML2 cells died rapidly in 1–2 days (Fig. 1d,e, Supplementary Fig. 5a), but THP-1 (Fig. 1f) and NOMO-1 cells (Supplementary Fig. 5b) required 5 days of compound treatment to achieve maximal cell killing. As expected, no cell death was observed in HEK293T and K562 cells even after 5 days of Val-boroPro treatment (Supplementary Fig. 5c,d).

We next wanted to characterize the mechanism of DPP8/9 inhibitor-induced pyroptosis in these human cells, and in particular identify the factors that determine cell sensitivity and resistance. We first asked which genes' expression levels are most correlated with sensitivity. This analysis, whether performed with the RNA microarray data from Cancer Cell Line Encyclopedia (CCLE) [17] across all of the cell lines (Fig. 2a), or only across the hematopoietic cell lines (Supplementary Fig. 6a), identified caspase-1 mRNA expression as a top predictor of Val-boroPro sensitivity. In contrast, the mRNA expression levels of DPP8 and DPP9 were not statistically different between sensitive and resistant cell lines (Supplementary Fig. 6b,c), indicating that the caspase-1 expression level, but not DPP8/9 expression levels, is a key determinant of cell sensitivity to Val-boroPro. Indeed, we found that pro-caspase-1 protein is expressed in the sensitive AML cell lines (Fig. 2b). Treatment of these cells with Val-boroPro induced cleavage of the pyroptotic substrate gasdermin D (GSDMD) and not the apoptotic substrate polyADP-ribose polymerase (PARP), demonstrating pyroptotic cell death (Fig. 2c). We confirmed that caspase-1 is required for cytotoxicity, as caspase-1 knockout OCI-AML2 (Fig. 2d,e), MV4;11 (Supplementary Fig. 7a,b), and THP-1 cells[1] (Supplementary Fig. 7c,d) were resistant to Val-boroPro and L-*allo*-Ile-isoindoline. In addition, we found that ectopic expression of caspase-1 in *CASP1*$^{-/-}$ THP-1 re-sensitizes the cells to Val-boroPro (Supplementary Fig. 7c,d). Pro-caspase-1 is typically activated by proximity-induced autoproteolysis into mature caspase-1 in ASC-containing inflammasomes, but pro-caspase-1 itself can be activated independent of ASC and without autoproteolysis to induce pyroptosis[18–20]. DPP8/9 inhibitors activate pro-

caspase-1 independent of ASC, and this form of active pro-caspase-1 cleaves GSDMD to induce pyroptosis but does not as efficiently cleave itself or pro-IL-1β[1]. Indeed, no cleavage of pro-caspase-1 or pro-IL-1β was observed in any of the AML cell lines (Supplementary Fig. 7e,f). We speculate that the involvement of pro-caspase-1, rather than mature caspase-1, might explain the slow kinetics of DPP8/9 inhibitor-induced pyroptosis (days) compared to canonical pathogen-induced pyroptosis (hours). In contrast to the sensitive cell lines, we observed little, if any, detectable pro-caspase-1 protein in the five Val-boroPro-resistant AML cell lines (Fig. 2b). Three of these cell lines, HEL, K562, and TF-1, were derived from erythroleukemias, and their low level of caspase-1 expression is consistent with their lineage, as caspase-1 expression is lowest in normal erythroid cells (Supplementary Fig. 6d)[21,22]. As expected, we observed no GSDMD cleavage after Val-boroPro treatment in the resistant cells, and K562 cells do not even express GSDMD (Fig. 2c). Intriguingly, HT-1080 fibrosarcoma cells expressed moderate levels of pro-caspase-1 protein but were not sensitive to Val-boroPro. We hypothesized these cells might lack another key protein in the pathway, for example the protein activator of pro-caspase-1.

We next wanted to identify the activator of human pro-caspase-1. We predicted the human pathway would be similar to the mouse pathway[3], and therefore that DPP8/9 inhibition would activate NLRP1, the human homolog of the mouse Nlrp1b. hNLRP1 and mNlrp1b have similar domain organizations, with nucleotide-binding (NACHT), leucine-rich repeat (LRR), “function-to-find” (FIIND), and CARD domains, although hNLRP1 contains an N-terminal pyrin domain (PYD) not present in mNlrp1b (Fig. 3a)[23]. To determine if hNLRP1 was required for DPP8/9 inhibitor-induced pyroptosis, we generated *NLRP1*$^{-/-}$ THP-1 and MV4;11 cell lines (Supplementary Fig. 8a). Surprisingly, we found that Val-boroPro induced pyroptosis in all of these *NLRP1*$^{-/-}$ cells (Supplementary Fig. 8b,c), demonstrating that NLRP1 is not required for DPP8/9 inhibitor-induced pyroptosis in humans. Intriguingly, the human genome, but not the mouse genome, encodes a protein, CARD8, that is similar to the C-terminal region of NLRP1, comprised of a FIIND followed by a CARD (Fig. 3a). CARD8 and NLRP1 are the only human proteins containing FIINDs[24]. The CARD of CARD8 is known to bind to the CARD of caspase-1 and induce caspase-1 activation [25,26], but the biological function of CARD8 has not yet been established. We next generated *CARD8*$^{-/-}$ THP-1, MV4;11, and OCI-AML2 cell lines, and found that these lines were all completely resistant to Val-boroPro, as no GSDMD cleavage or cell death was observed (Fig. 3b–d). These data indicate that CARD8 and pro-caspase-1 are required for DPP8/9 inhibitor-induced pyroptosis in these cells. Consistent with a requirement for CARD8 in DPP8/9 inhibitor induced pyroptosis, CARD8 protein is highly expressed in Val-boroPro sensitive AML cell lines, but is not expressed in pro-caspase-1 expressing, yet Val-boroPro resistant HT-1080 cells (Fig. 2b). We should note that, although NLRP1 does not mediate DPP8/9 inhibitor-induced pyroptosis in the cells tested here, these data do not exclude the possibility that NLRP1 mediates for DPP8/9 inhibitor-induced pyroptosis in different cell types or cell states.

We next wondered if CARD8 and caspase-1 expression is sufficient to confer sensitivity to DPP8/9 inhibitors. We therefore transiently transfected CARD8 or NLRP1 into HEK 293T cells stably expressing human caspase-1 and gasdermin D (to induce pyroptosis and not apoptosis[2]), and then treated these cells with Val-boroPro. We found that expression of

CARD8, but not NLRP1, rendered the cells sensitive to Val-boroPro-induced cytotoxicity (Fig. 3e,f). The FIIND of NLRP1 undergoes autoproteolytic cleavage[24], and this cleavage is required for activation of murine Nlrp1b by Val-boroPro[3] and anthrax lethal toxin[27]. Similarly, the FIIND of CARD8 also undergoes autoproteolytic cleavage[24] and is required for Val-boroPro-induced activation, as autoproteolytic-deficient S297A mutant CARD8 did not confer sensitivity to Val-boroPro (Fig. 3e,f). Like the activation of mNlrp1b by DPP8/9 inhibitors, proteasome inhibition blocks the activation of CARD8 (Fig. 3g). In this experiment, cells were only treated for 6 h rather than 24 h due to the induction of apoptosis by bortezomib over longer intervals. Interestingly, we observed a marked disappearance of the N-terminal fragment of CARD8 after Val-boroPro treatment (Fig. 3b–d,e), particularly in OCI-AML2 cells and in HEK 293T transfections. In contrast, more of the C-terminal fragment remained. Overexpression of the C-terminal region of CARD8, but not the N-terminal region, is toxic to HEK 293T cells expressing caspase-1 (Fig. 3h). We speculate that DPP8/9 inhibitors induce proteasomal degradation of the CARD8 N-terminus, freeing the C-terminus to activate pyroptosis, but the details of this mechanism warrant future study. Overall, these data indicate that CARD8 and CASP1 expression are sufficient for DPP8/9 inhibitor-induced cytotoxicity.

These data suggest that DPP8/9 inhibitors, in addition to eliciting indirect anti-tumor immune responses, might also have direct anti-cancer activity against AML *in vivo*. We therefore tested the efficacy of Val-boroPro against disseminated MV4;11 leukemia cells in immunodeficient non-obese diabetic–severe combined immunodeficient (NOD–SCID) Il2rg $^{-/-}$ (NSG) mice. In this model, MV4;11 cells stably expressing the firefly luciferase gene were injected into the tail vein of mice. Five days after inoculation, animals were randomized into control and treatment groups, and animals in the treatment group were given a Val-boroPro regimen that was well tolerated by immunocompetent mice in previous studies[7,8]. The two groups had similar disease burdens at the start of treatment (Supplementary Fig. 9a). Val-boroPro afforded a 97% reduction in tumor burden relative to the vehicle control at the end of drug treatment as measured by bioluminescence (Fig. 4a,b, Supplementary Fig. 9b). In addition, Val-boroPro-treated mice experienced a significant increase in survival over control-treated animals (Fig. 4c, 24.5-day median extension in survival, $p = 0.005$, log-rank test). This efficacious dosing was well tolerated, as we observed no significant effects on peripheral blood cell counts, serum chemistry, or body weight in these mice (Supplementary Fig. 9c–f). In similarly dosed wild-type C57BL/6J mice, we similarly observed no significant effects on peripheral blood counts or body weight (Supplementary Fig. 10). To confirm that the *in vivo* efficacy of Val-boroPro was due to pyroptosis of the cancer cells themselves, we performed a similar experiment using *CASP1*$^{-/-}$ MV4;11 leukemia cells. Val-boroPro had absolutely no efficacy against these cells *in vivo* (Fig. 4d,**e**), thereby establishing caspase-1 mediated pyroptosis of the AML cells as the basis for the *in vivo* efficacy. We next tested the efficacy of the more selective, albeit less potent, DPP8/9 inhibitor compound **8j**[28] in this leukemia model. We found that **8j** significantly inhibited leukemia progression (Supplementary Fig. 11), further confirming that DPP8/9 are the key targets mediating this response.

Primary AMLs express the highest median level of caspase-1 mRNA of all cancer types assessed in The Cancer Genome Atlas (TCGA) (Supplementary Fig. 12a) [29,30]. Moreover, high caspase-1 expression in AML is correlated with lower overall survival (Supplementary Fig. 12b) [22,31], indicating that caspase-1 is likely present in cancers with poor prognoses. Similar to the AML cell lines, we found that primary AML cells were sensitive Val-boroPro (Supplementary Fig. 13a,b). We confirmed that caspase-1 and CARD8 proteins are present in primary AML samples (Supplementary Fig. 14a,b), and that Val-boroPro induced cleavage of GSDMD into its pyroptotic p30 fragment without any evidence of apoptotic PARP cleavage (Supplementary Fig. 14b). As expected, no pro-caspase-1 cleavage was observed in any of the primary AML samples. We next determined the impact of Val-boroPro in a patient-derived xenograft (PDX) model of AML (categorized as FAB M1 AML, see Supplementary Table 3 for molecular characterization). After 10 days of dosing, Val-boroPro significantly reduced the number of human AML cells in peripheral blood by ~75% relative to the vehicle control (Fig. 4f). Moreover, Val-boroPro slowed weight loss associated with leukemia progression in this PDX model (Fig. 4g).

Collectively, these data indicate that selective inhibition of DPP8/9 is sufficient for cytotoxic activity against AML, and argues for the development of a potent and selective DPP8/9 inhibitor as a therapeutic agent for AML. An important caveat, however, is that the mechanism of action of DPP8/9 inhibitors in humans (CARD8) is different than their mechanism of action in mice (Nlrp1b), and therefore mouse models may not accurately predict the therapeutic window of DPP8/9 inhibitors in humans. For example, DPP8/9 inhibitors may induce pyroptosis in more or different primary cell lineages in humans and in mice. Although we found that non-AML human cancer cell lines (Fig. 1, Supplementary Table 2) and primary T-ALLs (Supplementary Fig. 14b,c) were completely resistant to Val-boroPro, primary human B-ALL (Supplementary Fig. 14d,e) and primary human cord blood CD34+ cells (Supplementary Fig. 14f) were sensitive to Val-boroPro. This may indicate that B-ALLs are also amenable to pyroptosis-mediated killing, but it could also suggest increased toxicity in humans compared with mice. Regardless, Val-boroPro reached serum concentrations in humans above the IC_{50} of human AML cells (>100 nM) without reaching a maximum tolerated dose[9], indicating that Val-boroPro itself is potentially a viable anti-AML agent. A more selective DPP8/9 inhibitor, or dosing DPP8/9 inhibitors after depleting hematopoietic cells (as would be achieved with the standard of care for AML[32]), might further mitigate potential toxicities as well.

In summary, here we have discovered that CARD8 mediates DPP8/9 inhibitor-induced pyroptosis in human myeloid cells. Although CARD8 has long been implicated in innate immunity, this the first report that CARD8 acts as an “inflammasome” sensor to activate caspase-1 in response to a specific stimulus. The anticancer potential of this pathway, which includes both direct cytotoxicity to AML cells and indirect induction of immune responses to solid tumors, warrants future investigations.

METHODS

Cloning

sgRNAs were designed using the Broad Institute's web portal [33] (http://www.broadinstitute.org/rnai/public/analysis-tools/sgrna-design) and cloned into the lentiGuide-Puro vector (Addgene #52963) as described previously[34]. The sgRNA sequences are listed in Supplementary Table 4. cDNA coding for full length human *CASP1* (Origene) was cloned with a C-terminal HA tag into pInducer20 vector (Addgene) and with a stop codon into a modified version of the pLEX_307 vector (Addgene) with a hygromycin resistance marker using Gateway technology (Thermo Fisher Scientific). cDNA coding for full length human GSDMD (Dharmacon) was cloned into the pLEX_307 vector (Addgene) with a C-terminal V5 tag. cDNAs coding for full length NLRP1 and CARD8 were purchased from Origene and RFP from Addgene and cloned with stop codons into the pLEX_307 vector. The C-terminal and N-terminal region of CARD8 were cloned with stop codons into pLEX_307 and pDEST27, respectively. The S297A single amino acid point mutation was generated with the QuickChange site-directed mutagenesis kit (Agilent).

Reagents and antibodies

Val-boroPro[35], 1G244[13], L-*allo*-Ile-isoindoline[12], 8j[28], and 5385[1] were synthesized according to previously published protocols. For cell culture experiments, Val-boroPro was resuspended in DMSO containing 0.1% TFA to prevent compound cyclization. For *in vivo* experiments, Val-boroPro was resuspended and stored in sterile 0.01 M HCl at a concentration of 2 mg/mL. Immediately before *in vivo* administration, the 2 mg/mL stocks of sterile Val-boroPro were diluted to 20 μg/100 μL in sterile PBS (pH = 7.4). LPS was purchased from Santa Cruz Biotechnology, nigericin and doxycycline from the Cayman Chemical Company, bortezomib from LC Laboratories, etoposide from Enzo Life Sciences, and sitagliptin from Sigma. Antibodies used were: hCD45 (#304036, BioLegend, V510 conjugate, clone HI30), hCD45 (#304012, BioLegend, APC conjugate, clone HI30), mCD45 (#103108, BioLegend, FITC conjugate, clone 30-F11), hCD3 (#300440, BioLegend, FITC conjugate, clone UCHT1), hCD3 (BE0231, BioXCell, clone UCHT1), hCD33 (#366618, Biolegend, PECy7 conjugate, clone P67.6), human caspase-1 (#2225, Cell Signaling Technology), DPP9 (ab42080, Abcam), GAPDH (clone 14C10, Cell Signaling Technology), GSDMD (NBP2-33422, Novus Biologicals), IL-1β (Clone 2805, R&D Systems), PARP (#9542, Cell Signaling Technology), NLRP1 (AB_10891878, R&D Systems), CARD8 N-term (#ab194585, Abcam), and CARD8 C-term (#ab24186, Abcam).

Cell culture

A375, HEK 293T, THP-1, RS4;11, HT-1080, Jurkat, U937, and MCF-7 cells were purchased from ATCC. SET-2, HL-60, KG1, MOLM-13, MV4;11, NOMO1, NB4, OCI-AML2, OCI-AML3, HEL, KASUMI-1, TF-1, and K562 cells were purchased from DSMZ. DAOY, IMR5, ONS-76, RD-ES, and TC71 cells were gifts from Johannes Schulte and were verified using STR genotyping (Genetica DNA Laboratories). HEK 293T, DAOY, HT-1080, IMR, JURKAT, MCF-7, ONS-76, RDES, and TC71 cells were grown in Dulbecco's modified Eagle's medium (DMEM) with 10% fetal bovine serum (FBS). THP-1, RS4;11, HL-60, KG1 MOLM-13, MV4;11, NOMO1, NB4, OCI-AML2, HEL, KASUMI-1, K562,

U937 SET2, and Jurkat cells were grown in RPMI-1640 medium with 10% FBS. $CD45^+$ human cord blood (CB) cells (StemCell Technologies, Catalog 70008.3) were thawed in IMDM with 15% FBS and DNase1 (1 mg/mL) and grown in IMDM supplemented with 10% FBS, 1 × penicillin/streptomycin, 100 ng/mL TPO, 100 ng/mL SCF, and 100 ng/mL G-CSF. All cells were grown at 37 °C in a 5% CO_2 incubator. Cell viability assays were performed on CB cells immediately after thawing. Cell lines were tested for mycoplasma using the MycoAlert™ Mycoplasma Detection Kit (Lonza).

CellTiter-Glo cell viability assay

Cells were plated (2000 cells/well) in white, 384-well clear bottom plates (Corning) using an EL406 Microplate Washer/Dispenser (BioTek) in 25 μL final volume of media. Compounds were added using a pintool (CyBio). MV4;11, RS4;11, and CB cells were incubated for 22 h and all other cells were incubated for 46 h at 37 °C. Assay plates were then removed from the incubator and allowed to equilibrate to room temperature on the bench top before addition of 10 μL of CellTiter-Glo reagent (Promega) according to the manufacturer's instructions. Assay plates were shaken on an orbital shaker for 2 minutes and incubated at room temperature on the bench top for 10 minutes. Luminescence was then read using a Cytation 5 Cell Imaging Multi-Mode Reader (BioTek).

LDH cytotoxicity assays

Cells were seeded at 1.0×10^6 cells/well in 6-well plates in standard growth medium and treated with DMSO, Val-boroPro, and/or bortezomib. After the indicated time, supernatants were harvested and analyzed for LDH activity using an LDH cytotoxicity assay kit (Pierce). For the ectopic expression caspase-1 in *CASP1*$^{-/-}$ THP-1 cells, doxycycline (1μg/mL) was added when cells were transferred to 6-well plates. DMSO or Val-boroPro was added together with doxycycline, re-dosed after 24 h, and LDH release was analyzed after 48h. For experiments involving HEK 293T cells, cells were seeded at 0.5×10^6 cells/well in 6-well plates in DMEM containing 10% FBS one day prior to transfection. Cells were then transiently transfected with the indicated plasmid DNA (if less than 2 μg was used, then the total DNA was normalized to 2 μg the RFP vector) with using the Fugene HD transfection reagent (Promega), treated as described, and supernatants and cell lysates were collected at the time indicated. Supernatants were analyzed for LDH activity using the Pierce LDH Cytotoxicity Assay Kit (Life Technologies) according to the manufacturer's instructions. The HEK 293T lysates were also used for immunoblotting experiments.

Primary cancer cell assays

Primary cancer specimens (except AML-10) were collected from patients treated at the Memorial Sloan Kettering Cancer Center. Patients provided informed consent to the study, which was approved by the MSKCC IRB. AML-10 was collected by Champions Oncology (Baltimore, MD). Primary samples were collected by bone marrow aspirate from consenting patients on protocol 09-141. After bone marrow aspiration, the bone marrow aspirate was passed through a 100 μM cell strainer and washed with 1X PBS. The cell suspension was layered over Ficoll-Paque PLUS and centrifuged at 1000 × g for 20 minutes. Bone marrow mononuclear cells (BM MNCs) at the interphase were transferred to a new conical tube and

washed with 1X PBS. BM MNCs were resuspended in 5 mL of ACK and incubated on ice for 5 minutes. 15 mL of 1X PBS was added to stop lysis and the remaining cell suspension was centrifuged at 400 RCF (4°C) for 10 minutes. Cells were resuspended in 1X PBS, counted, and frozen. For AML samples 1–4, purified mononuclear AML cells were transplanted in non-obese diabetic–severe combined immunodeficient (NOD–SCID) *Il2rg*$^{-/-}$ (NSG) mice (The Jackson Laboratory) and engrafted primary AML cells were harvested and cryopreserved, as previously described [36]. The other primary samples were used directly from patients for *in vitro* studies. Primary cancer cells were thawed in Iscove's Modified Dulbecco's Medium (IMDM) with 15% FBS and DNase1 (1 μg/mL) and grown in culture media consisting of IMDM with 15% FBS, 1× penicillin/streptomycin (Corning), 0.1 mM 2-mercaptoethanol, 20 ng/mL G-CSF (Peprotech 300-23), 100 ng/mL SCF (PeproTech 300-07), 20 ng/mL IL-3 (PeproTech 200-03), 50 ng/mL FLT3-Ligand (PeproTech 300-19). For cytotoxicity analysis, cells were plated in a 96-well plate (Corning 3903) one day after thawing at a density of 100,000 cells in 100 μL per well. Each cell line was treated with Val-boroPro (20 μM) or DMSO in triplicate and incubated for 40 hours at 37 °C. After 40 hours, cells were washed with 2.5% FBS in 1×PBS and stained with anti-mouse CD45 (FITC), anti-human CD45 (APC), and PI (Fisher Scientific) or DAPI (ThermoFisher Scientific). Stained cells were sorted using a BD FACSCanto II instrument (BD Bioscience) and data were analyzed using FACSDiva (BD Bioscience) and FlowJo software. The gating strategy for flow cytometry is shown in Supplementary Figure 16.

Immunoblotting experiments

Cell lines (1.0×10^6 cells) were seeded in 6-well plates and treated with DMSO or compounds as described. THP-1 cells were also treated with LPS (10 μg/mL) for 24 h. After 24 h, LPS-primed cells were treated with nigericin (20 μM) for 30 minutes. For primary cell western blots, primary cells were thawed and seeded in 6 well plates at $3 \times 10^6 – 4 \times 10^6$ cells/well. Seeded primary cells were treated with DMSO or Val-boroPro for 24 h. Cells were washed 2x in PBS (pH = 7.4), resuspended in PBS, and lysed by sonication. Protein concentrations were determined using the DCA Protein Assay kit (Bio-Rad). The samples were separated by SDS-PAGE, immunoblotted, and visualized using the Odyssey Imaging System (Li-Cor).

Generation of stable cell lines

For generation of knockout cell lines: constructs were packaged into lentivirus in HEK 293T cells using the Fugene HD transfection reagent (Promega) and 2 μg of the vector, 2 μg psPAX2, and 0.2 μg pMD2.G. Target cells were spinfected with virus for 1 h at 1000*g* at 30 °C supplemented 8 μg/mL polybrene. After 2 days, cells were selected for stable expression of S. pyogenes Cas9 (Addgene #52962) using blasticidin (5 μg/mL for MV4;11, MOLM-13, and OCI-AML2; 1 μg/mL for THP-1) and for stable expression of sgRNAs using puromycin (0.5 μg/mL for OCI-AML2 and THP-1; 1 μg/mL for MV4;11 and MOLM-13). After 10 d, the cells were harvested for immunoblotting or experiments. For isolation of complete knockouts, single cells were isolated by serial dilution and expanded. For the over expression of proteins: For the generation of bioluminescent MV4;11 cells: the PMMP-luc-neo retroviral plasmid (6 μg) was transfected into HEK293T cells with the packaging vectors pMD.MLV (1.5 μg) and pCMV-VSV-G (1.5 μg) using the Fugene HD

transfection reagent. MV4;11 cells were spin infected with viral particles at an MOI = 1 for 1 hour at 2500g at 37°C supplemented with 8 μg/mL polybrene. After 2 days, firefly luciferase expressing cells were selected with neomycin (2 mg/mL) for 14 days. For the ectopic expression of *CASP1* and GSDMD, the expression plasmid (2 μg) was transfected into HEK293T cells with the packaging vectors psPAX2 (2 μg) and VSVG (0.2 μg) using FugeneHD transfection reagent. After 2 days, THP-1 *CASP1* knockout or HEK 293T cells were spinfected with virus particles for 1 hour at 1000g at 30°C supplemented with 8 μg/mL polybrene. After 2 days, THP-1 CASP1 expressing cells were selected with G418 (200 μg / mL), HEK 293T CASP1 expressing cells were selected with hygromycin (200 μg /mL), and HEK 293T GSDMD expressing cells were selected with puromycin (1 μg /mL).

Gene expression analysis

Gene expression data was obtained from the Cancer Cell Line Encyclopedia (CCLE) (https://portals.broadinstitute.org/ccle/home) [17], and genes distinguishing sensitive and resistant cell lines were identified with a two-class comparison using Morpheus (https://software.broadinstitute.org/morpheus/).

Annexin V and PI staining

1×10^6 cells were treated with DMSO, Val-boroPro (2 μM), or etoposide (50 μM) for 24h. The cells were then analyzed using the Annexin V-FITC Apoptosis Kit (Clontech) according to the manufacturer's protocol. The gating strategy for flow cytometry is shown in Supplementary Figure 16.

In vivo studies

All mouse experiments with MV;411 cells were performed at the MSKCC animal facility and approved by the institutional animal care and use committee. One million MV4;11-Luc Neo cells were injected into the tail vein of sub-lethally (200 cGy) irradiated 7-week-old female non-obese diabetic–severe combined immunodeficient (NOD–SCID) *Il2rg*$^{-/-}$ (NSG) mice (The Jackson Laboratory). For the Val-boroPro experiment with wild-type MV4;11 cells: five days after injection, the mice were randomly grouped (n = 9 mice per group) and treated intraperitoneally with 100 μL of vehicle (1 mM HCl in PBS, pH = 7.4) or 100 μL of VbP (20 μg/ 100 μL) once daily, 5 days a week for 4 weeks. Animals were weighed daily. Tumor burden was measured on the indicated days by BLI using an IVIS Spectrum system (Caliper Life Sciences). After 23 days of drug dosing, peripheral blood from 3 mice per group (high, median, and low total flux BLI readings) was obtained and analyzed for complete blood counts and blood chemistry by MSKCC Antitumor Assessment Core and Laboratory of Comparative Pathology, respectively. The femur, spleen, lung, and liver from these mice were also harvested, embedded in paraffin, sectioned at 5μm and stained with haematoxylin and eosin (sectioning and staining was performed by MSKCC Antitumor Assessment Core and the Molecular Cytology Core). Survival analysis was measured from the time of cancer inoculation to the moribund state (6 mice per group), and Prism 7 software (Graph Pad) was used for statistical analysis. We selected 9 mice per group so that we could perform blood and tumor burden analysis on 3 mice and have six mice for survival analysis, similar in size to previous studies using this model [37]. For the Val-boroPro experiment with *CASP1*$^{-/-}$ MV4;11 cells: the experiment was performed as described for

wild-type MV4;11 cells, except dosing was stopped after 3 weeks due to a lack of efficacy and survival analysis was performed using all 9 animals. For the 8j experiment: five days after tumor injection, the mice were randomly grouped (n = 6 mice per group) and treated intraperitoneally with 100 μL of vehicle (1% DMSO in PBS) or 100 μL of 8j (600 μg/ 100 μL) once daily, 5 days a week for 4 weeks. Tumor burden was determined as described above. To evaluate Val-boroPro in C57BL/6J mice, 7-week-old female C57BL/6J mice (The Jackson Laboratory) were treated with vehicle (1 mM HCl/PBS) or Val-boroPro (20 μg) once (n=5 per group, harvested at 6 h or 24 h) or once daily, five days a week for two weeks (10 doses, n=4, harvested 24 h after last treatment). Blood was collected from the mice and was analyzed for complete blood count and complete blood chemistry. The AML-10 PDX mouse model was performed by Champions Oncology approved by their institutional animal care and use committee. AML cells were thawed at 37°C, and diluted to 1×10^6 AML cells per 0.2 ml volume and stored on ice. OKT3 (BioXCell) was diluted to a 1-mg/mL solution in sterile PBS containing 2% FBS and stored at 4°C until use. OKT3 antibody was incubated with cells in suspension on ice for 30 minutes at a concentration of 1 μL/1 million WBC (1 μg/million) just prior to IV injection. Ten 5-week-old female NOD.Cg-Prkdcscid Il2rgtm1Sug/JicTac (NOG; Taconic #NOG-F) were irradiated at 175 cGy and injected with 1×10^6 AML cells via tail vain. After 5 weeks, peripheral blood (~200 μL) was stained for CD33 (PECy7), CD45 (V510), and CD3 (FITC) and analyzed by FACS to confirm leukemia engraftment. Engrafted mice were split into two groups (n=5 per group), and treated with either vehicle (0.01 M HCl/PBS) or Val-boroPro (2 mg/kg) for 28 days (5 days per week for 4 weeks). After 10 and 28 days of dosing, the leukemia burden in the peripheral blood was determined by FACS analysis. This study was not designed to monitor overall survival. No animals were excluded. The investigators were not blinded.

EnPlex assay

Selectivity profiles were determined by EnPlex as described previously [15].

Statistical analysis

Two-sided Student's *t* tests were used for significance testing unless stated otherwise. *P* values less than 0.05 were considered to be significant. Graphs and error bars represent means ± SEM of independent biological experiments unless stated otherwise. The investigators were not blinded in all experiments. All statistical analysis was performed using GraphPad Prism 7. Additional information about statistical analysis and reproducibility is available in the Life Sciences Reporting Summary.

Supplementary Material

Refer to Web version on PubMed Central for supplementary material.

Acknowledgments

We thank S. Monette for histology advice, and W. Bachovchin, W. Wu, and J. Lai for Val-boroPro, 1G244, 8j, and L-*allo*-Ile-isoindoline. This work was supported by the Josie Robertson Foundation (D.A.B and A.K.), a Stand Up to Cancer-Innovative Research Grant (Grant Number SU2C-AACR-IRG11-17 to D.A.B.; Stand Up to Cancer is a program of the Entertainment Industry Foundation. Research Grants are administered by the American Association for Cancer Research, the scientific partner of SU2C), the Pew Charitable Trusts (D.A.B. is a Pew-Stewart Scholar in

Cancer Research), the NIH (R01 AI137168 to D.A.B.; R21 CA188881 and R01 CA204396 to A.K.; T32 GM115327-Tan to D.C.J.; the MSKCC Core Grant P30 CA008748), the American Cancer Society (Postdoctoral Fellowship PF-17-224-01 – CCG to C.Y.T.), Borroughs Wellcome Fund (A.K), Alex's Lemonade Stand Foundation (A.K.), Gabrielle's Angel Foundation (A.K.), and the Damon Runyon Cancer Research Foundation (A.K. is the Damon Runyon-Richard Lumsden Foundation Clinical Investigator).

References

1. Okondo MC, et al. DPP8 and DPP9 inhibition induces pro-caspase-1-dependent monocyte and macrophage pyroptosis. Nat Chem Biol. 2017; 13:46–53. [PubMed: 27820798]
2. Taabazuing CY, Okondo MC, Bachovchin DA. Pyroptosis and Apoptosis Pathways Engage in Bidirectional Crosstalk in Monocytes and Macrophages. Cell Chem Biol. 2017; 24:507–514. e504. [PubMed: 28392147]
3. Okondo MC, et al. Inhibition of Dpp8/9 Activates the Nlrp1b Inflammasome. Cell Chem Biol. 2018
4. Zhang H, Chen Y, Keane FM, Gorrell MD. Advances in understanding the expression and function of dipeptidyl peptidase 8 and 9. Mol Cancer Res. 2013; 11:1487–1496. [PubMed: 24038034]
5. Rosenblum JS, Kozarich JW. Prolyl peptidases: a serine protease subfamily with high potential for drug discovery. Curr Opin Chem Biol. 2003; 7:496–504. [PubMed: 12941425]
6. Wagner L, Klemann C, Stephan M, von Horsten S. Unravelling the immunological roles of dipeptidyl peptidase 4 (DPP4) activity and/or structure homologue (DASH) proteins. Clin Exp Immunol. 2016; 184:265–283. [PubMed: 26671446]
7. Adams S, et al. PT-100, a small molecule dipeptidyl peptidase inhibitor, has potent antitumor effects and augments antibody-mediated cytotoxicity via a novel immune mechanism. Cancer Res. 2004; 64:5471–5480. [PubMed: 15289357]
8. Walsh MP, et al. Val-boroPro accelerates T cell priming via modulation of dendritic cell trafficking resulting in complete regression of established murine tumors. PLoS One. 2013; 8:e58860. [PubMed: 23554941]
9. Cunningham CC. Talabostat. Expert Opin Investig Drugs. 2007; 16:1459–1465.
10. Eager RM, et al. Phase II trial of talabostat and docetaxel in advanced non-small cell lung cancer. Clin Oncol (R Coll Radiol). 2009; 21:464–472. [PubMed: 19501491]
11. Eager RM, et al. Phase II assessment of talabostat and cisplatin in second-line stage IV melanoma. BMC Cancer. 2009; 9:263. [PubMed: 19643020]
12. Lankas GR, et al. Dipeptidyl peptidase IV inhibition for the treatment of type 2 diabetes: potential importance of selectivity over dipeptidyl peptidases 8 and 9. Diabetes. 2005; 54:2988–2994. [PubMed: 16186403]
13. Jiaang WT, et al. Novel isoindoline compounds for potent and selective inhibition of prolyl dipeptidase DPP8. Bioorg Med Chem Lett. 2005; 15:687–691. [PubMed: 15664838]
14. Wu JJ, et al. Biochemistry, pharmacokinetics, and toxicology of a potent and selective DPP8/9 inhibitor. Biochem Pharmacol. 2009; 78:203–210. [PubMed: 19439267]
15. Bachovchin DA, et al. A high-throughput, multiplexed assay for superfamily-wide profiling of enzyme activity. Nat Chem Biol. 2014; 10:656–663. [PubMed: 24997602]
16. Spagnuolo PA, et al. Inhibition of intracellular dipeptidyl peptidases 8 and 9 enhances parthenolide's anti-leukemic activity. Leukemia. 2013; 27:1236–1244. [PubMed: 23318959]
17. Barretina J, et al. The Cancer Cell Line Encyclopedia enables predictive modelling of anticancer drug sensitivity. Nature. 2012; 483:603–607. [PubMed: 22460905]
18. Broz P, von Moltke J, Jones JW, Vance RE, Monack DM. Differential requirement for Caspase-1 autoproteolysis in pathogen-induced cell death and cytokine processing. Cell Host Microbe. 2010; 8:471–483. [PubMed: 21147462]
19. Guey B, Bodnar M, Manie SN, Tardivel A, Petrilli V. Caspase-1 autoproteolysis is differentially required for NLRP1b and NLRP3 inflammasome function. Proc Natl Acad Sci U S A. 2014; 111:17254–17259. [PubMed: 25404286]
20. Van Opdenbosch N, et al. Activation of the NLRP1b inflammasome independently of ASC-mediated caspase-1 autoproteolysis and speck formation. Nat Commun. 2014; 5:3209. [PubMed: 24492532]

21. Novershtern N, et al. Densely interconnected transcriptional circuits control cell states in human hematopoiesis. Cell. 2011; 144:296–309. [PubMed: 21241896]
22. Bagger FO, et al. BloodSpot: a database of gene expression profiles and transcriptional programs for healthy and malignant haematopoiesis. Nucleic Acids Res. 2016; 44:D917–924. [PubMed: 26507857]
23. Ting JP, et al. The NLR gene family: a standard nomenclature. Immunity. 2008; 28:285–287. [PubMed: 18341998]
24. D'Osualdo A, et al. CARD8 and NLRP1 undergo autoproteolytic processing through a ZU5-like domain. PLoS One. 2011; 6:e27396. [PubMed: 22087307]
25. Agostini L, et al. NALP3 forms an IL-1beta-processing inflammasome with increased activity in Muckle-Wells autoinflammatory disorder. Immunity. 2004; 20:319–325. [PubMed: 15030775]
26. Razmara M, et al. CARD-8 protein, a new CARD family member that regulates caspase-1 activation and apoptosis. J Biol Chem. 2002; 277:13952–13958. [PubMed: 11821383]
27. Frew BC, Joag VR, Mogridge J. Proteolytic processing of Nlrp1b is required for inflammasome activity. PLoS Pathog. 2012; 8:e1002659. [PubMed: 22536155]
28. Van Goethem S, et al. Inhibitors of dipeptidyl peptidase 8 and dipeptidyl peptidase 9. Part 2: isoindoline containing inhibitors. Bioorg Med Chem Lett. 2008; 18:4159–4162. [PubMed: 18556198]
29. Cerami E, et al. The cBio cancer genomics portal: an open platform for exploring multidimensional cancer genomics data. Cancer Discov. 2012; 2:401–404. [PubMed: 22588877]
30. Gao J, et al. Integrative analysis of complex cancer genomics and clinical profiles using the cBioPortal. Sci Signal. 2013; 6:pl1. [PubMed: 23550210]
31. Cancer Genome Atlas Research N et al. Genomic and epigenomic landscapes of adult de novo acute myeloid leukemia. N Engl J Med. 2013; 368:2059–2074. [PubMed: 23634996]
32. Khwaja A, et al. Acute myeloid leukaemia. Nat Rev Dis Primers. 2016; 2:16010. [PubMed: 27159408]
33. Doench JG, et al. Optimized sgRNA design to maximize activity and minimize off-target effects of CRISPR-Cas9. Nat Biotechnol. 2016; 34:184–191. [PubMed: 26780180]
34. Sanjana NE, Shalem O, Zhang F. Improved vectors and genome-wide libraries for CRISPR screening. Nat Methods. 2014; 11:783–784. [PubMed: 25075903]
35. Coutts SJ, et al. Structure-activity relationships of boronic acid inhibitors of dipeptidyl peptidase IV. 1. Variation of the P2 position of Xaa-boroPro dipeptides. J Med Chem. 1996; 39:2087–2094. [PubMed: 8642568]
36. Wang K, et al. Patient-derived xenotransplants can recapitulate the genetic driver landscape of acute leukemias. Leukemia. 2016
37. Daigle SR, et al. Selective killing of mixed lineage leukemia cells by a potent small-molecule DOT1L inhibitor. Cancer Cell. 2011; 20:53–65. [PubMed: 21741596]

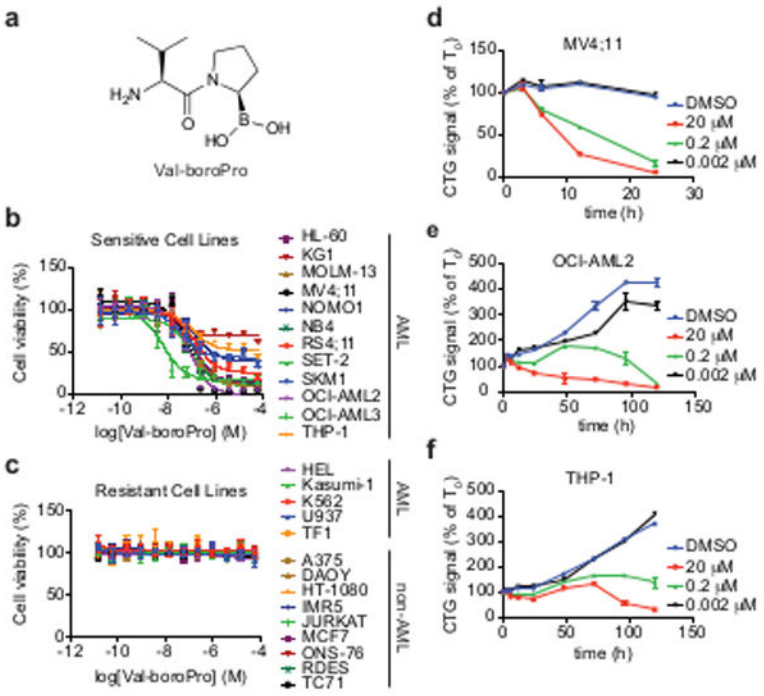

Figure 1. Val-boroPro is cytotoxic to AML cells

(**a**) The structure of Val-boroPro. (**b**,**c**) Dose response of cell viability of sensitive (**b**) and resistant (**c**) cell lines to treatment with Val-boroPro (24 h for MV4;11 and RS4;11 cells, 48 h for all others) relative to DMSO. (**d–f**) Time-course of cell viability of MV4;11 (**d**), OCI-AML2 (**e**), and THP-1 (**f**) cells after treatment with DMSO or Val-boroPro at the indicated concentrations. Data are means ± SEM of three biological replicates.

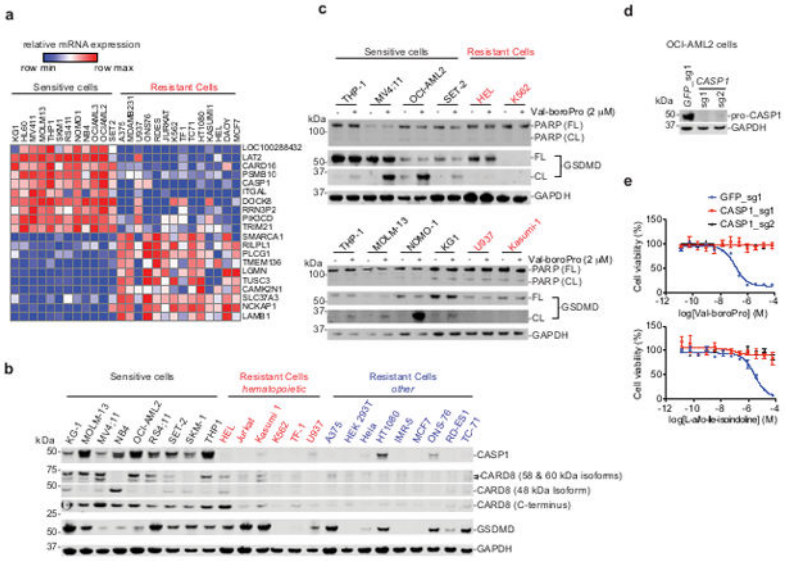

Figure 2. Caspase-1 is required for the sensitivity of AML cell lines to Val-boroPro

(**a**) Genes whose level of expression (from CCLE microarray data[17]) distinguishes between cell lines that are sensitive and resistant to Val-boroPro. The twenty genes whose expression levels are most highly correlated with sensitivity and resistance are shown. Each row corresponds to a gene and each column corresponds to its relative expression levels in each cell line. The top ten genes are highly expressed in sensitive cells lines, and the bottom ten genes are highly expressed in resistant cell lines. (**b**) Immunoblots of lysates from the indicated sensitive and resistant cell lines, showing levels of CASP1, CARD8, GSDMD, and the loading control GAPDH. (**c**) Immunoblots of lysates from AML cell lines treated with or without Val-boroPro for 24 h, showing levels of full-length (FL) and cleaved (CL) PARP and GSDMD. See Supplementary Figure 7 for immunoblots for caspase-1 and IL-1β. Immunoblots in **b** and **c** are representative of >5 independent experiments. (**d**) Immunoblots of lysates from OCI-AML2 cells treated with sgRNAs to *CASP1* or to *GFP* (control). Images are representative of 3 independent experiments. (**e**) Cell viability of control and caspase-1 knockout OCI-AML2 cells after treatment with the indicated concentrations of Val-boroPro (**d**) or L-*allo*-Ile-isoindoline (**e**) at 24 h. Data are means ± SEM of three independent biological experiments. Full gel images of cropped gels are shown in Supplementary Figure 15.

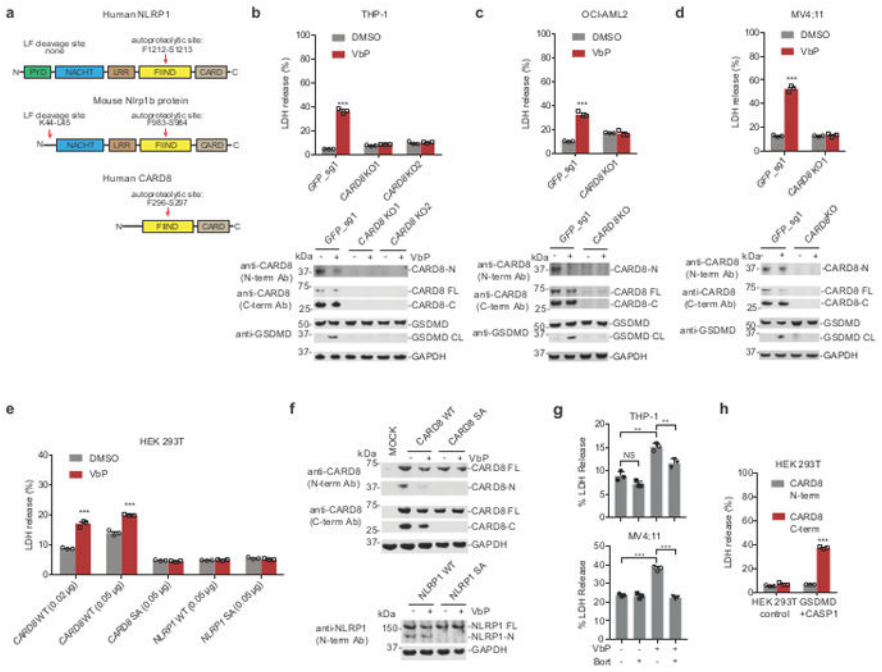

Figure 3. CARD8 mediates DPP8/9 inhibitor-induced pyroptosis in human myeloid cells

(**a**) Diagram of human NLRP1, mouse Nlrp1b (allele 1), and human CARD8 proteins. The lethal factor (LF) cleavage and FIIND autoproteolysis sites are indicated. The FIIND-CARD regions of CARD8 and NLRP1 are ~44% identical. The cartoon is not drawn to scale. (**b–d**) Top, percentage of LDH release (relative to the amount of LDH released by 0.36% Triton X-100, which lyses all cells) from *CARD8* KO THP-1 (**b**), OCI-AML2 (**c**), and MV4;11 (**d**) cells after treatment with DMSO or Val-boroPro (VbP; 2 μM; 24 h for OCI-AML2 and MV4;11, 48 h for THP-1). Bottom, immunoblots showing levels of CARD8 and GSDMD. Antibodies that bind specifically to either the CARD8 N-terminus or the CARD8 C-terminus were used as indicated. N, N-terminus; C, C-terminus; FL, Full-length, CL, cleaved. Immunoblots in **b–d** are representative of 3 independent experiments. (**e**) Percentage of LDH release from HEK 293T cells stably expressing hCASP1 and hGSDMD that were then transiently transfected with the indicated constructs, followed 24 hours later by treatment with DMSO or Val-boroPro (2 μM) for an additional 24 hours. (**f**) Immunoblots of lysates of cells from **e** (0.05 μg transfection). Cells transiently transfected with a vector encoding RFP were used as a mock. Immunoblots in are representative of >5 independent experiments. (**g**) Percentage of LDH release from THP-1 or MV4;11 cells were treated for 6 h with DMSO, Val-boroPro (2 μM), bortezomib (100 nM), or both Val-boroPro and bortezomib. (**g**) Percentage of LDH release from HEK 293T cells or HEK 293T cells stably expressing hCASP1 and hGSDMD 24 hours after transient transfection with the indicated constructs. Data in **b–e**, **g**, and **h** are means ± SEM of three independent biological experiments. **p < 0.01, ***p < 0.001 by two-sided Student's *t*-test. NS, not significant (p > 0.05).

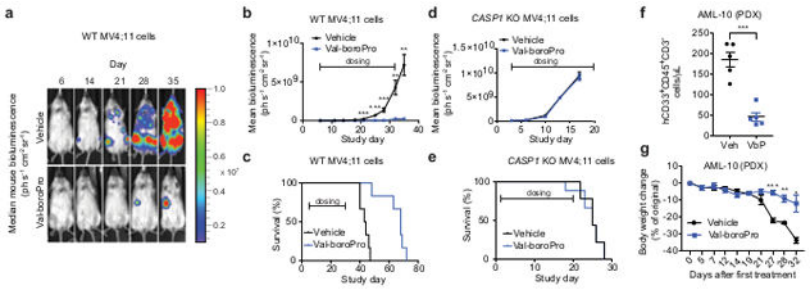

Figure 4. Val-boroPro inhibits AML progression *in vivo*

(**a–c**) Bioluminescent images (**a**), mean bioluminescence over the time course of the study (n=9 mice per group) (**b**), and Kaplan-Meier survival analysis (n=6 mice per group, p=0.0005, two-sided log-rank test) (**c**) of mice bearing wild-type MV4;11 leukemia cells treated with vehicle (1 mM HCl/PBS) or Val-boroPro. Mouse with the median bioluminescence in each group is shown in **a**. (**d**,**e**) Mean bioluminescence (**d**) and Kaplan-Meier survival analysis (**e**) of mice bearing *CASP1* knockout MV4;11 leukemia cells treated with vehicle or Val-boroPro (n=9 mice per group). The results for the vehicle- and drug-treated groups are not statistically different in **d** (p=0.68, two-sided Student's *t*-test on study day 17) or **e** (p=0.9086, two-sided log-rank test). (**f**) Total number of human viable AML cells expressing CD45 and CD33 and not expressing CD3 in peripheral blood of mice bearing primary human cancer AML-10 that were treated with vehicle or Val-boroPro (n=5 mice per group). The total number of cells was determined by FACS analysis 10 days after the start of treatment. (**g**) Mean body weights of mice in the PDX model in **f**. Data in **b**, **d**, **f,** and **g** are means ± SEM. *p < 0.05, **p < 0.01, ***p < 0.001 by two-sided Student's *t*-test.